Slov Vet Res
DOI 10.26873/SVR-2342-2026

Early View

Original Research Article

Novel Discovery of *Ossa Cordis* in the Reticulated Giraffe (*Giraffa reticulata*)

Key words

calcium;
collagen;
microscopy;
trabeculation;
X-ray computed microtomography

Craig J Sturrock[1], Adam Best[2], Aziza Alibhai[2], Jorja Jackson-Oxley[2], Jennie J Jeyapalan[2], Brian Atkinson[1], William Perez[3], Catrin Sian Rutland[2]*

[1]The Hounsfield Facility, School of Biosciences, University of Nottingham, Leicestershire, LE12 5RD, [2]School of Veterinary Medicine and Science, Faculty of Medicine and Health Sciences, University of Nottingham, Leicestershire, LE12 5RD, United Kingdom, [3]PEDECIBA, Universidad de Montevideo, Montevideo, Uruguay

***Corresponding author:** catrin.rutland@nottingham.ac.uk

Abstract: *Ossa cordis* and *cartilago cordis* are heterotopic bone and cartilage, respectively, in the cardiac skeleton of the heart. Relatively few species have *cartilage cordis*, an even smaller number have *ossa cordis*, and very few observations of cartilage surrounding *ossa cordis* have been published. In species presenting with *ossa cordis*, the prevalence, anatomical location, histological structure, architecture, number of *ossa cordis* per heart, existence of cartilage circumventing the bone, and links to cardiovascular disease vary between species, and between individuals of the same species. The current, novel, research utilized X-ray computed microtomography (μCT) in the cardiac skeleton of the reticulated giraffe (*Giraffa reticulata,* formally *Giraffa camelopardalis reticulata*). A giraffe *ossa cordis* has also never been observed using histological and microscopic methods. Therefore, haematoxylin and eosin (H&E), special stains Von Kossa (indicating calcium deposits), Alcian blue pH 0.2 and 2.5 (indicating acidic polysaccharides, such as glycosaminoglycan present in cartilage) and immunohistochemistry alongside light microscopy, and Picrosirius red (indicating collagen) with polarized light microscopy accompanied the μCT study. This research established the size, shape and microstructure, including bone thickness throughout the giraffe *ossa cordis* using dissection and μCT. The types of bone and cartilage were identified using histological methods, and detailed microstructure aspects including collagen quantity and types, vasculature and disease status. This work also explored the theories relating to endochondral and intramembranous ossification. Importantly, this case study described giraffe *ossa cordis* shape, size, microstructures and histological features for the first time.

Received: 11 June 2026
Accepted: 17 July 2026

Introduction

In adult mammals, the left and right sides of the heart are divided by interatrial and interventricular septa between the atria and ventricles respectively. The four chambers are surrounded by internal supporting fibrous tissue (cardiac skeleton) and myocardium (1). The cardiac skeleton (also termed the cardiac fulcrum in people) is a fibrous structure made up of collagen and elastin fibers which act to maintain the hearts shape during systole (2-6). In mammals, the cardiac skeleton consists of two trigones, left and right, each incorporating an atrioventricular ring (6, 7). The cardiac skeleton may contain dystrophic calcification (also referred to as plaques), cartilage including fibrocartilage and hyaline cartilage (*cartilago cordis*) and, on occasion, bone (*ossa cordis*) (7, 8). Abnormal, benign formation of bone within soft tissues where bone does not normally exist, is termed heterotopic ossification, a process frequently triggered by systemic changes (9). Whilst it is often related to pathology, this is not always the case. *Ossa cordis* are considered heterotopic bones, which are hypothesized to develop via endochondral ossification or intramembranous ossification, or a combination of both (7). Endochondral ossification occurs via the calcification of cartilage and which, in turn, usually develops into cancellous bone and eventually mature bone. Intramembranous ossification, in contrast, occurs when mesenchymal cells differentiate into osteoblasts which then produce bone tissue directly (6, 10). Both of these processes are naturally occurring during skeletal development, bone remodeling and repair.

In general, bone, when fully developed, may contain trabecular bone and cortical (lamellar/compact) bone, which may be surrounded by periosteum. *Ossa cordis* is similar but rarely has a periosteum, and trabeculation and marrow are not always present (7). Bone tissues exhibit three main cell types (osteocytes, osteoblasts and osteoclasts), in addition to vasculature containing endothelial cells and smooth muscle, these features have been noted in many *ossa cordis* publications. Cartilage contains no vasculature or nervous tissue and is mostly composed of chondrocytes

within a ground substance of mainly collagen, this is the same for *cartilago cordis* (8). It has been hypothesized that endocardial ossification contributes towards the formation of *ossa cordis*, as cartilage surrounding the bone has been observed in a few species and some species can contain both *cartilago cordis* and *ossa cordis* (6, 8, 11-13).

The *ossa cordis* in the giraffe has been known about for some years. In the 1800s three anatomists stated the presence of *ossa cordis* in giraffes following dissection. Following the dissection of one whole Nubian (*Giraffa camelopardalis camelopardalis*) male, and parts of one male and one female giraffe (subspecies and ages not specified) a description was provided of *ossa cordis* (14). Owen stated that the *ossa cordis* was located at the base of the heart, near the origin of the aorta, imbedded in the tendinous circle attaching to the muscular fibres of the ventricle in the adult giraffe. It is not stated whether this was in all three hearts, or just the whole male dissected. Two other papers implied or stated the presence of an *ossa cordis* in giraffes – these were in undetermined subspecies, ages, sexes, and numbers of specimens (15, 16). In a more recent case study, a single *ossa cordis* in the right fibrous trigone of a *Giraffa camelopardalis rothschildi* (17). This was alongside a 'tiny structure consisting of hyaline cartilage' (*cartilago cordis*) in the left fibrous trigone in the giraffe heart (17). The aims of these previous publications concentrated on overall anatomical descriptions of cardiovascular structures or the whole body, therefore the *ossa cordis* and *cartilago cordis* were noted during the dissections, and no histological or imaging methods were applied to any of the *ossa cordis* or *cartilago cordis*.

The present study investigated an endangered, reticulated giraffe (*Giraffa reticulata*) presenting with an *ossa cordis*. Computed tomography and microtomography (µCT) has only been used more recently to investigate *ossa cordis*, firstly in the chimpanzee (11), then in cattle and camels (18-20). Therefore, the present study used µCT to visualize the *ossa cordis* within cardiac skeleton of the giraffe. This research also used a variety of histological stains, visualized with brightfield and polarized light microscopy, to explore the microstructure and composition of the *ossa cordis*, surrounding ectopic cartilage, and adjacent myocardial tissue. This novel study therefore provides the first µCT and histological investigation into the giraffe *ossa cordis*.

Materials and methods

Ethics and sample collection

All research included in this thesis received ethical approval from the University of Nottingham School of Veterinary Medicine and Science ethics committee under UK approved ethical guidelines (ethics number: 3186 200604). The giraffe died following a medical procedure (non-research purposes). Following death, the giraffe underwent a postmortem examination and was subsequently received by the University of Nottingham. The male, adult, captive bred, reticulated giraffe (*Giraffa reticulata*) was 11 years old, had an estimated weight of 1000kg and had a heart weight of 5.147kg. The heart was fixed in 10% neutral buffered formalin.

µCT

Working from apex to base, the heart was finely resected and palpated for hyperdense tissues. The interatrial septum contained dense material therefore this region was excised and µCT scanned as conducted previously (11, 20). The tissue was secured in sheets of X-ray transparent polyethylene and placed in a plastic sample container. Using a Waygate Technologies 'v|tome|x M' 240 kV cone beam X-ray µCT scanner, the specimen was scanned with a tube energy of 120 kV and 100 µA current, collecting 180 projection images over a 360° rotation. Each projection image was the integration of 4 images to reduce noise using a detector timing of 250 ms per image. The scan resolution was 15 µm and the scan time was approximately 40 minutes. Imaging data from the µCT was visualised using VGStudioMAX v2.2 Software (Volume Graphics GmbH, Germany). Mean local thickness for the bone within the ossa cordis was also measured using the BoneJ plugin for the open-source image quantification and analysis software ImageJ 1.44 following previous protocols (11, 21-23). Localised variation of bone density was measured by mapping the variation in image grayscale values which relate to the X-ray attenuation of the material using VGStudioMAX (e.g. higher density materials have higher X-ray attenuation and thus higher grayscale values). The local thickness heat map images were imported into VGStudioMax and visualised.

Tissue processing and embedding

Following µCT scans, five tissue samples were dissected from the cardiac skeleton, hyperdense (*ossa cordis*) region and neighbouring myocardium. Half of the *ossa cordis* was photographed following soft tissue removal, the other half was processed for histological staining with the surrounding myocardial tissue intact. In addition, atrial septum tissue not containing bone/cartilage was also excised, then processed for histology. All tissues were dehydrated in a series of ethanol solutions (VWR International Limited, USA) for at two hours each (50, 70, 90 and 100%) followed by xylene (VWR International Limited, USA) for two hours. All samples were immersed in 60°C paraffin wax for four hours, then mounted in a paraffin block and sectioned at 7 µm using a microtome (Leica, Germany) and N35 blades. For each sample, up to 300 serial sections of tissue were mounted onto polysilinated microscope slides (Fisher Scientific, UK). Slides were dried on a 50 °C heat plate followed by 24 hours at room temperature. Prior to staining, sections were deparaffinised in xylene (VWR International Limited, USA) for five minutes then rehydration in a graded ethanol series (100, 90, 80, 70%; VWR International Limited, USA) followed by dH_2O, then phosphate buffered saline (all five minutes each). Following staining, sections were dehydrated in graded ethanols (70, 80, 90, 100%; VWR International Limited, USA) for five minutes each and coverslips mounted using DPX mounting media (Merck Life Sciences, UK).

Staining, immunohistochemistry and microscopy

Hematoxylin and Eosin (H&E): Sections were incubated in hematoxylin (Merck Life Sciences, UK) for three minutes, washed in tap water for three minutes, then incubated in industrial methylated spirit solution (VWR International Limited, USA) for 15 seconds. Sections were then washed in tap water for three minutes, incubated in 1% ammoniated water for 15 seconds, then washed once more, in tap water for three minutes. Sections were incubated in eosin (Merck Life Sciences, UK) for five minutes followed by a final three-minute wash in tap water then dH_2O.

Alcian blue: For pH 0.2 Alcian blue staining, 0.3 g of solid Alcian blue (J60122, Alfa Aesar, USA) was mixed with 30ml of 10% sulphuric acid to produce a 1% solution of pH 0.2 Alcian blue stain. Sections were incubated in the pH 0.2 Alcian blue solution for 15 minutes. For pH 2.5 Alcian blue staining, sections were incubated in 3% acetic acid for five minutes before being incubated in a commercially available pH 2.5 alcian blue stain (MKCL4108, Sigma-Aldrich, USA) for 30 minutes. Sections were washed in tap water for five minutes. All pH 0.2 and pH 2.5 sections were then rinsed in deionized water for one minute, counterstained with nuclear fast red for one minute, followed by a one-minute tap water wash.

Von Kossa: Von Kossa staining was performed using a commercially available kit (HC993161, Merck Millipore, Germany) as conducted previously (11). Sections were incubated in 0.1M silver nitrate solution for 20 minutes then placed under direct light for another 20 minutes. Sections were washed in tap water for three minutes before being incubated in sodium thiosulphate (20 g/L) for five minutes, then washed in tap water for a minute.

Picrosirius red: Tissue sections were incubated for one hour with Picrosirius red stain (ab150681, Abcam, UK), washed twice with acetic acid, then submerged in 100% ethanol (VWR International Limited, USA) for 10 minutes as conducted previously (11, 24, 25). Imaging and quantification were also conducted following previous protocols (11, 24) using Fiji software (26) to calculate the area coverage of coloured pixels, which was calculated into proportions using Microsoft Excel (Microsoft Corp. USA).

Immunohistochemistry: Immunohistochemistry was performed using an anti-osteocalcin primary antibody (also called bone gamma-carboxyglutamate BGLAP; ab93876; Abcam, UK) as conducted previously (27). Following deparaffinization and rehydration of the tissues, antigen retrieval was undertaken in 1mM sodium citrate, microwaved for 20 minutes, allowed to cool for 20 minutes then washed in dH_2O for 5 minutes. Immunohistochemistry was performed using a commercially available diaminobenzidine based kit (7150-K, Leica Biosystems, Germany) according to the manufacturer's protocol. Sections were either exposed to the primary antibody (1:100) or the buffer only (5% fetal calf serum) to serve as negative controls. A positive control containing mouse bone and skeletal tissue was also conducted. Sections were counterstained in hematoxylin.

Microscopy: All sections were visualized using a Leica DM5000 B microscope (Leica, Germany). Standard brightfield was used for all stains except for Picrosirius red which required polarized light. A brightfield light slide scanner (NanoZoomer S60v2, Hamamatsu, Japan), was also used with images viewed on NDP.view2Plus (https://www.hamamatsu.com/eu/en/product/life-science-and-medical-systems/digitalslide-scanner/U12388-01.html; Hamamatsu Photonics K.K., Japan).

Phylogenetic tree

A published systematic review (7) plus updated literature searches were used to collate species containing *ossa cordis*, and the reticulated giraffe was added to that data. Papers that did not specifically confirm *ossa cordis*, *cartilago cordis* or ectopic calcification (e.g. where only CT scans were completed without necessary histological confirmation of hyperdense CT material) were excluded from the tree. A phylogenetic tree was created using iTOL Interactive Tree of Life (https://itol.embl.de/) and PhyloT v2 (https://phylot.biobyte.de/) as conducted previously (8).

Results

Dissection, µCT observations

Within the giraffe, a single, rectangular shaped bone was present in the atrial septum in the right trigone (Figure 1+2+3B), no bone or cartilage was present in the rest of the atrial septum. The bone was classified as an *ossa cordis dextrum* based on the anatomical location and the combined µCT and histological findings. The *ossa cordis dextrum* measured 18.5 mm long, 7 mm wide and 7 mm deep at its maximum points (using µCT and caliper measurements; Figures 1, 2 and 3B). Total volume of solid material of the *ossa cordis* measured using µCT was 139.72 mm^3 and its surface area was 1399 mm^2. The µCT imaging identified trabeculations within the *ossa cordis*, a characteristic feature of bone (Figure 2, Supplementary Videos 1+2). There were also lower density regions between the trabeculations – identified as bone marrow in the histological examinations. The mean bone thickness was 0.227 mm (SD 0.09), however showed regions within both the cortical bone and trabeculae that ranged from 0.07 – 0.6 mm (Figure 2C, D). Bone density varied and ranged from 24000 – 65535 CT image gray value units, with a mean and standard deviation of 43837.5 and 5497.9, respectively (Figure 2E, F).

The phylogenetic tree construction illustrated the species with confirmed *ossa cordis*, including the reticulated giraffe as a novel species following these findings (Figure 3). In total, therefore, 22 species/subspecies now have a verified *ossa cordis* observed in at least one individual.

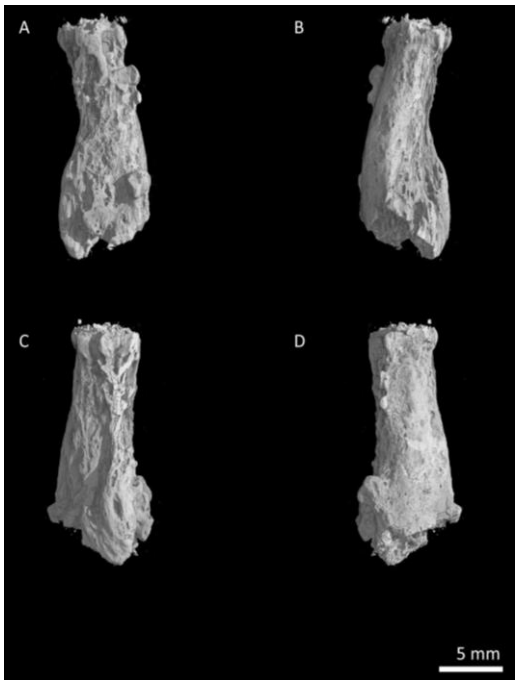

Figure 1: µCT images showing shape and structure of the giraffe ossa cordis. Surface rendered image of the giraffe ossa cordis. A) Ventrālis, B) Sinistral, C) Dorsālis, D) Dextral, at 120 kV, 100 µA, and scan resolution 15 µm. Scale bar represents 5 mm

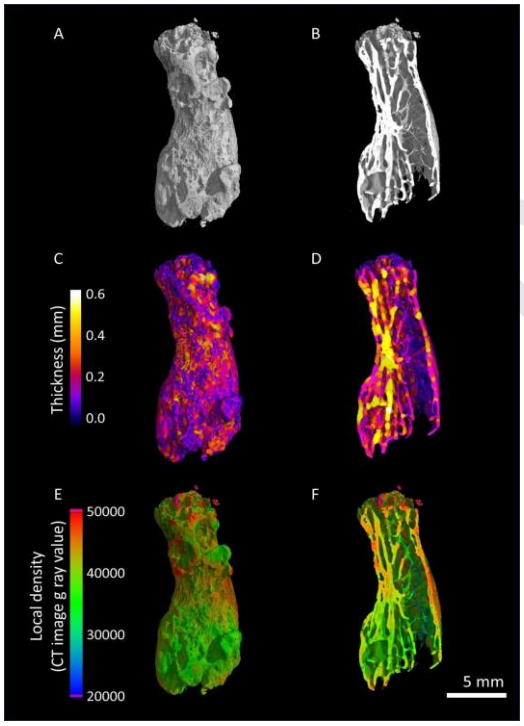

Figure 2: µCT images showing size, thickness, local density and trabeculations in the giraffe *ossa cordis*. Surface rendered image of the giraffe *ossa cordis* A) Ventrālis view and B) digital frontal section to reveal the trabeculations. C) Local thickness measurement heatmaps of the whole *ossa cordis* (Ventrālis view) and D) a digital frontal section to reveal the thickness of trabeculations (0 – 0.6 mm). E) Map of µCT image gray value variation as an indication of bone density variation of the *ossa cordis* (Ventrālis view) F) a digital frontal section to reveal the variation in density of trabeculations of the giraffe *ossa cordis*. Scale bar represents 5 mm

Histological observations

Within the heart tissue sections, cardiomyocytes within typically striated myocardium including blood vessels were observed. No evidence of heart disease was seen. The bone on the peripheral edges of the ossa cordis dextrum was cortical bone, composed of mature lamellar bone. Distinct bone marrow with adipose tissue was seen within the trabeculated *ossa cordis* structure (Figure 4), thus confirming the µCT findings of bone. Blood vessels were seen frequently on the peripheral edges of the bone tissue and on occasion within the bone marrow too (Figure 4). Histological observations confirmed chondrocytes and cartilage surrounding the peripheral cortical bone regions of the *ossa cordis dextrum*. Chondrocytes were, on occasion, seen adjacent to the bone tissue (Figure 4). Alcian blue staining at pH 0.2 stained a deep blue colour around cartilage, especially compared to pH 2.5 stained sections. Alcian blue was also seen in lighter shades within the bone tissue and myocardium (Figure 5). This suggested presence of acid mucins, notably glycosaminoglycans which are usually present in cartilage.

Von Kossa stained positively the bone tissue (Figure 5), indicating calcium deposits were present, further indicating bone tissue that was mineralised. In addition, the calcification was uniform across the *ossa cordis* (Figure 5) indicating more mature lamellar bone versus immature woven bone (which would show irregular calcification). Positive osteocalcin immunohistochemical staining was observed in the *ossa cordis*, vasculature and in the myocardial tissue (Figure 6).

The use of Picrosirius red allowed for analysis of collagen types within the bone and surrounding myocardium. The collagen fibres within the bone tissue were well organized, densely packed, usually in clear bundles running the same direction, again indicating mature lamellar bone as opposed to immature woven bone (Figure 7). The layers of unidirectional collagen bundles were evident throughout the *ossa cordis*. There was a distinct difference between the red/yellow staining of the bone and the more abundantly green staining in the surrounding myocardium (Figure 7). The bone was predominantly red/yellow, indicating type I collagen. The levels were so high in the *ossa cordis* (Figure 7A-H) itself that true quantitative analysis, looking at both collagen types (red/yellow versus green), was not possible due to the strong stain given by the red and yellow stained fibres. Quantitative analysis was possible regarding the myocardial tissue, immediately adjacent to bone and further away (Figure 7C-L). Microscopic observations showed lower levels of thicker red fibers (type I collagen) compared to green (type III) occurred in the myocardium around the periphery of bone/cartilage tissue. Ratios analysis showed 16% red fibers/84% green in the myocardium adjacent to the *ossa cordis*, whereas in the myocardium where the *ossa cordis* was not immediately adjacent, the percentage of red fibers (type I) increased to 42%, and the green fibers reduced to 58% green (type III; Figure 7L). The Picrosirus red staining, in addition to the other stains, also assisted with identifying the presence of a periosteum. There were also clear boundaries between the bone showing predominantly red/yellow staining (type I collagen) indicative of Sharpey fibres, and the predominantly green fibres (collagen type III) of the myocardium (especially evident in Figure 7C-G).

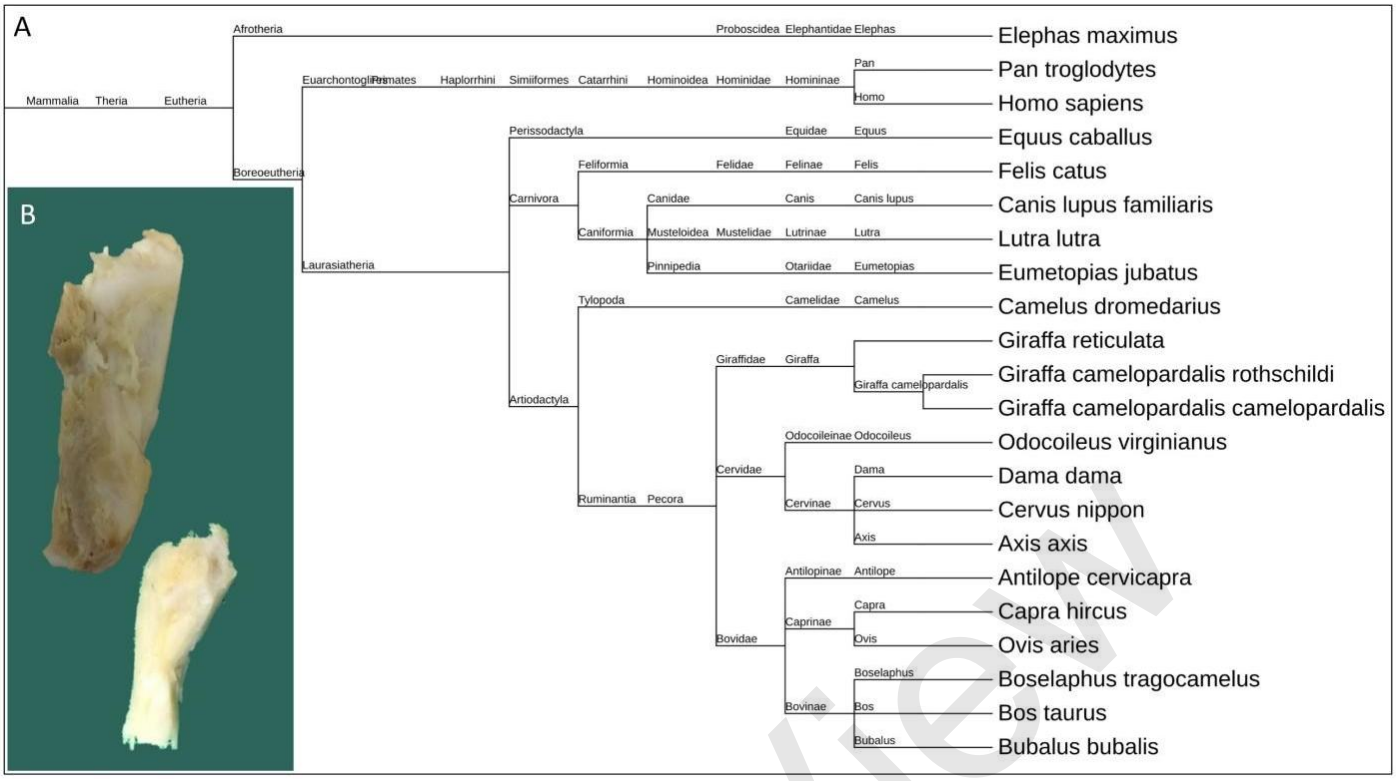

Figure 3: Gross structure of the giraffe *ossa cordis* and phylogenetic tree. A) Phylogenetic tree of species with confirmed *ossa cordis*. B) Photograph of the *ossa cordis* dissected from the interatrial septum, prior to (above), and following (below) soft tissue removal

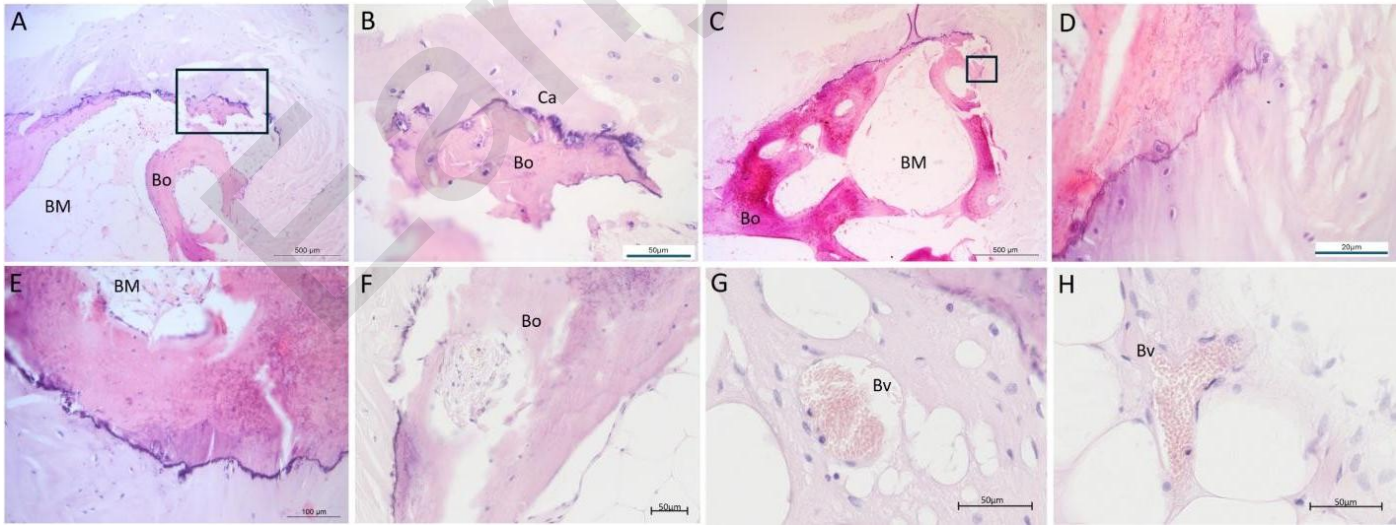

Figure 4: Giraffe *ossa cordis* with ectopic cartilage formation (H&E stained). Giraffe *ossa cordis* with bone evident (pink stain of eosin) with ectopic cartilage surrounding the *ossa cordis*, evidenced by chondrocytes (purple haematoxylin stain). This may indicate endochondral ossification as chondrocytes were observed invading bone tissue (indicated in the boxes within A+C and in B+D which are higher magnifications of A+C respectively). A, E, F) Bone marrow within *ossa cordis*. Scale bars represent A+C) 500µm, D) 20µm, E) 100µm. F-H) 50µm. BM = Bone marrow, Bo = bone, Bv = blood vessel, Ca = cartilage

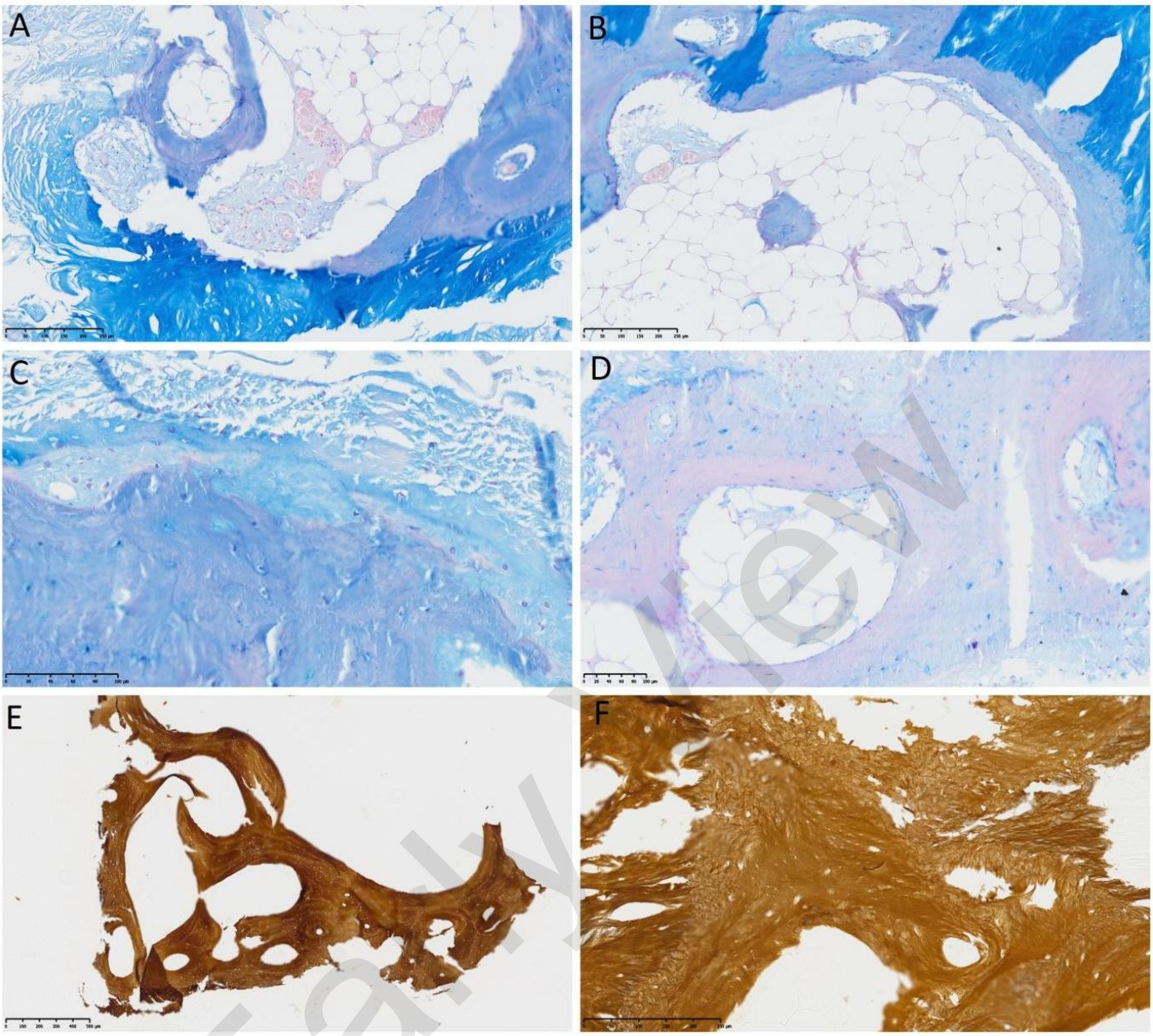

Figure 5: Giraffe *ossa cordis* following Alcian blue and Von Kossa staining. A-D) Alcian Blue at pH0.2 (A-C) and pH2.5 (D). E+F) Von Kossa silver nitrate. Scale bars represent: A, B, F) 250µm, C, D)100µm, E) 500µm

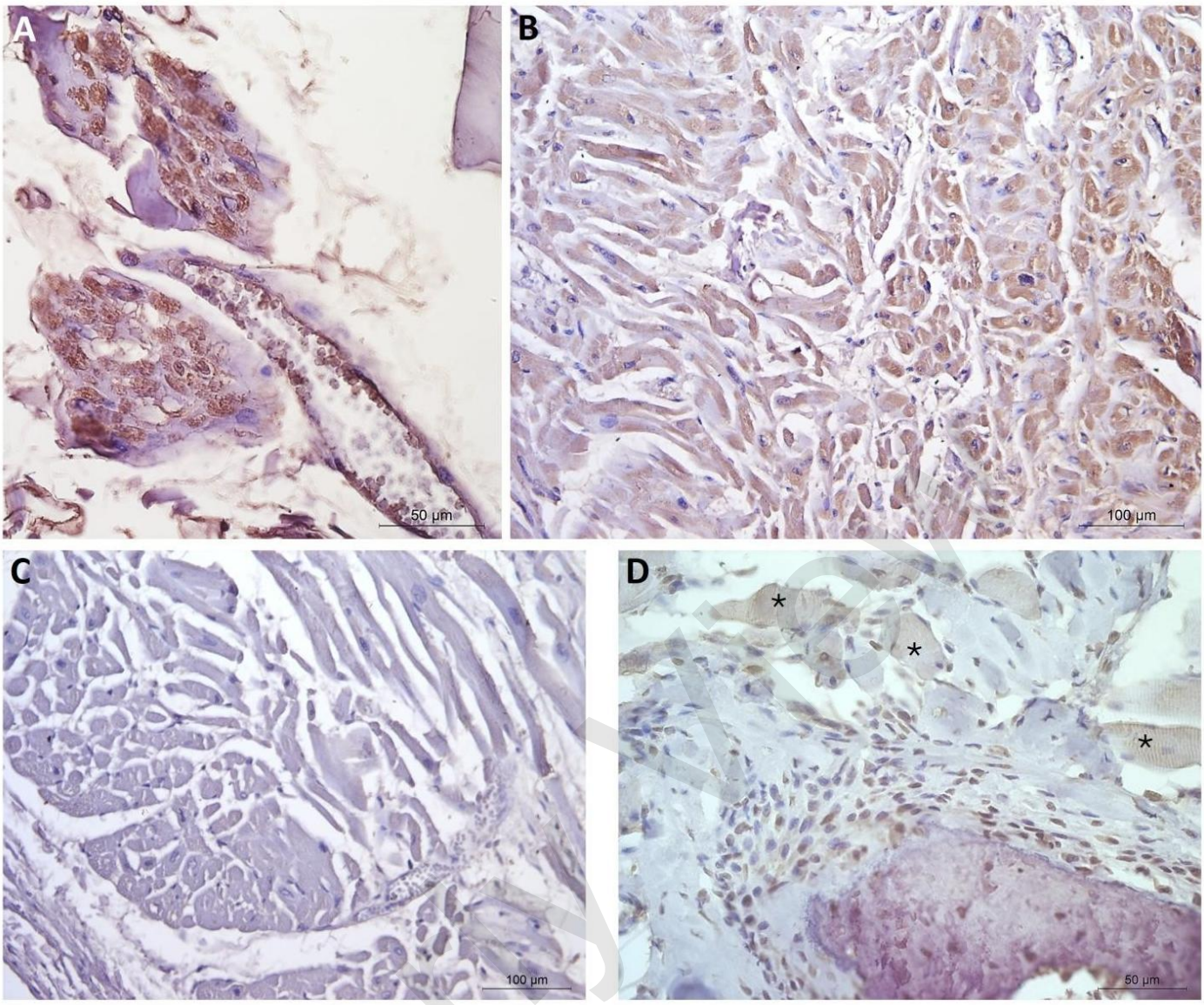

Figure 6: Giraffe *ossa cordis* following osteocalcin immunohistochemistry. A) Giraffe *ossa cordis* and blood vessel, B) Giraffe myocardium, (1:100 dilution), C) Giraffe negative control (primary antibody omitted). D) Mouse bone and skeletal muscle (asterix) positive control tissue. Scale bars represent A+D) 50µm, B+C) 100µm

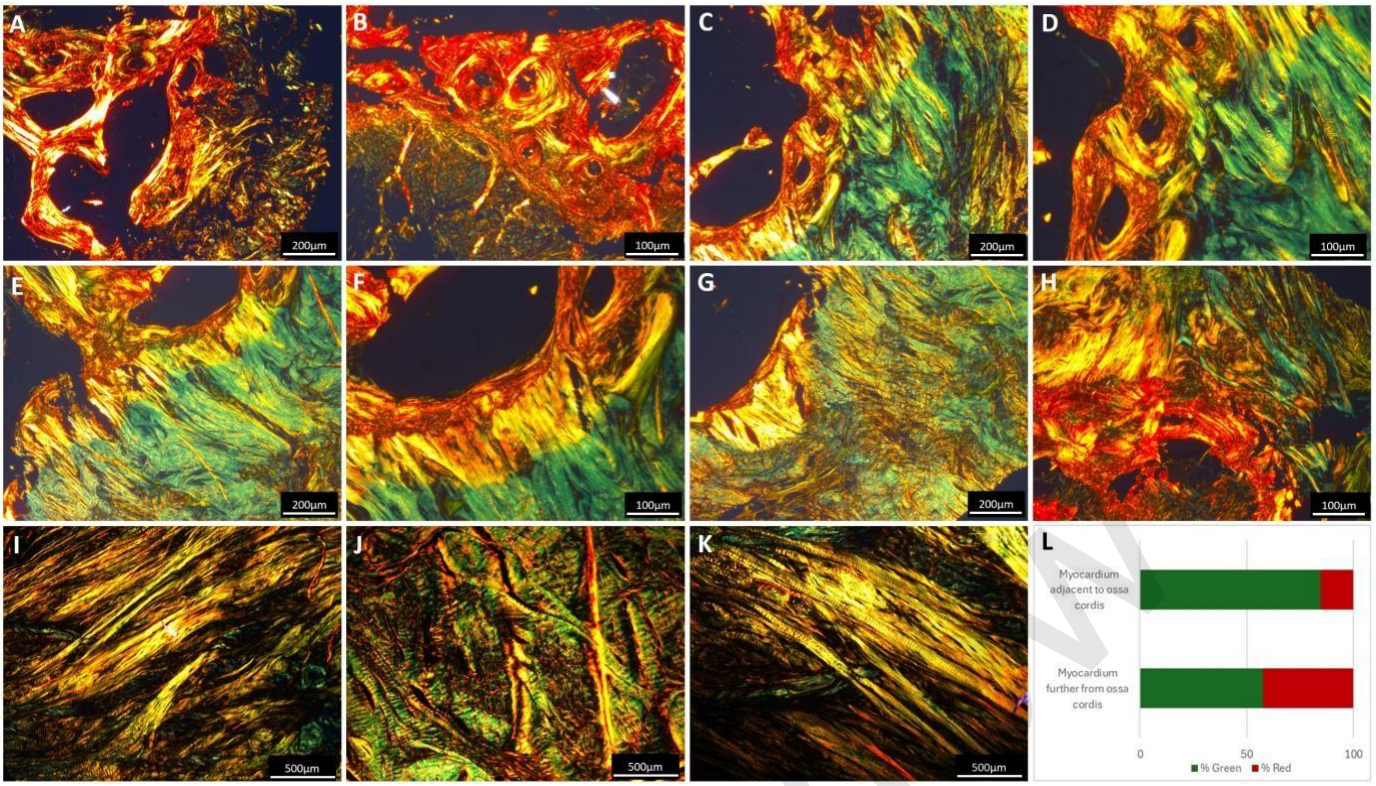

Figure 7: Picrosirius red staining on giraffe *ossa cordis* and myocardium. Red/yellow indicates collagen type I and green staining indicates collagen type III, under polarized light microscopy. A-H) Ossa cordis stained red/yellow following Picrosirius red stain. E-H) Myocardium directly attached to the bone presented as yellow staining with adjacent myocardium presented with more green staining. I-K) Myocardium further away from the bone presented with more red/yellow staining compared to myocardium adjacent to the bone. L) Percentage of red/yellow (collagen type I) versus green (collagen type III). Scale bars represent A, C, E, G) 200µm, B, D, F, H) 100µm, I-J 500µm

Discussion

The aim of this study was to investigate a giraffe heart cardiac skeleton for hyperdense tissue, and to identify whether *cartilago cordis*, *ossa cordis*, or cartilage surrounding *ossa cordis* presented in the heart. This is the first report of giraffe *ossa cordis* being investigated using radiographical and histological techniques with detailed morphological and histological details revealed. By using µCT alongside histological techniques it was possible to show that a single *ossa cordis dextrum* was present in the giraffe heart within the interatrial septum. Confirmation of an *ossa cordis* within the reticulated giraffe adds another species to the phylogenetic tree of animals containing *ossa cordis*, and another within the Artiodactyla order. The Atriodactyla order has many more species/subspecies, including the giraffe investigated in this study, with *ossa cordis* present compared to other phylogenetic orders (14/22 in Artiodactyla versus 8/22 from other mammalian orders). Notably all of the Artiodactyla order animals are within Pecora infraorder, except for the camel. This differs from the species variation observed in *cartilago cordis*, which has around 70 confirmed species with the structure but also more variation in relation to class, order, family, genus and species (8, 28-30). At present the mere observation that many species have *ossa cordis* in one order compared to others does not prove there is an evolutionary or genetic link to the occurrence of *ossa cordis*, more studies need to be completed in more species. It should also be noted that across most species where *ossa cordis* have been identified, they rarely occur in all of the individuals studied. There has been a range of 0-100% prevalence (7) and previous published works in the giraffes were either case studies or did not publish specimen numbers or prevalence (14-17). As the present study was a case study it would be interesting to gain a better comprehension of giraffe *ossa cordis* in a larger population in future research.

The present case study discovered a single *ossa cordis dextrum* in the giraffe. The previous, historical, dissection only observations, also indicated only *ossa cordis dextrum* (or assumed dextrum), not sinistrum, in adult giraffes (14-17). Notably, in one giraffe case study, a small cartilaginous structure in the left trigone was observed (17), this was not found in our specimen. The reticulated giraffe in the present study had one *ossa cordis dextrum* and did not have an *ossa cordis sinistrum*. This makes it similar to goats, cats, chimpanzees, sea lions, and dogs where a single *ossa cordis dextrum* has been observed (11, 31-33). Studies in other species that noted *ossa cordis sinistrum*, showed it was always in addition to *ossa cordis dextrum* (never instead of). Sheep, buffalo, cattle,

camels, deer, elephants and otters, can have both *ossa cordis dextrum* and *sinistrum* (12, 13, 18, 19, 34-38). It is essential to note the prevalence of the second bone (*ossa cordis sinistrum*) was not 100% in these species, and of course the presence of *ossa cordis dextrum* was rarely 100% either in any given species either (7). It is interesting that predominantly other members of the Artiodactyla order do have both *ossa cordis dextrum* and *sinistrum*, unlike this giraffe specimen. Given the *ossa cordis dextrum* plus cartilaginous tissue in one previous giraffe case (17), and the fact that prevalence is variable within all species, there is the possibility a full *ossa cordis sinistrum* may yet reside in other individual giraffes.

The reticulated giraffe *ossa cordis dextrum* measured 18.5 x 7 x 7 mm and was rectangular in shape. Owen stated that in the giraffe *ossa cordis* was a curved bone two-thirds of an inch in length, this equates to ~16.9 mm (14), whilst Crisp recorded a bone 'nearly an inch' (nearly ~25.4 mm) long in the adult giraffe (16). The number of specimens, species/subspecies, ages other than being adult, were not stated, but 18.5 mm was relatively similar to the sizes they observed. Murie and Perez did not state *ossa cordis* sizes or shapes in their giraffes (15, 17), but it must be noted none of these publications were *ossa cordis* focused manuscripts. In comparison to other species, the length of the *ossa cordis* in the present study was most similar to that found in an Iranian-breed sheep (39). It was smaller compared to the average sizes known for buffalo, cattle, sea lions, deer, elephants, and goats as previously presented (7). In contrast the giraffe *ossa cordis dextrum* was longer than that observed in otters, some sheep breeds and chimpanzees (11, 12, 36). Sadly, comparisons between all species were limited as not all published studies detailed size, however it does show that animals with much smaller heart weights and body masses had larger *ossa cordis* present compared to the giraffe. In general, *ossa cordis* have shown large variations in shape between species and even between individuals within the same species (7). Many publications do not state shape, predominantly due to the imaging modes used. The giraffe in the study looked more like a long bone (rectangular), whereas most are irregular and sometimes a little flat. Bones can be curved, Y shaped, oval to mainly elongated quadrilateral or rectangular with a pointed caudoventral end and a rounded cranial end (20), rounded and completely irregular (11, 12), elongated rectangular through to short or long elliptical (19) and triangular or elongated (38). The rectangular shape observed in the giraffe adds to the variability seen in *ossa cordis* shapes in different individuals.

Ossa cordis have been more prevalent in post-natal or adult, rather than embryonic and juvenile, individuals (7). The giraffe in the present study was 11 years old and approximately 44% through its average lifespan. Crisp and Murie saw no *ossa cordis* in the two independent 'juvenile/young' male cases studies, one aged 7 months, the other age not specified, they dissected independently (15, 16). Murie did not specify how many adult giraffes they dissected, or their sex, age or subspecies but he agreed with Crisp regarding the cardiac ossicle (*ossa cordis*) in adults (presumed present) and the juvenile (explicitly stated absent) (15). The presence of *ossa cordis* in the adults was not specifically by Murie, yet the absence in the juvenile was noted to be the exception compared to adults. Perez and Owen showed ossa cordis in their adult giraffes (14, 17). Despite the brevity of these observations, they do give an indication that *ossa cordis* were generally present in adult giraffes. The present study supports the presence of *ossa cordis* in another adult specimen but given this information, no conclusions can be drawn regarding the age of onset of *ossa cordis* in this species. Further research into younger individuals would help understand whether it develops *in utero*, or during later developmental stages. *Ossa cordis* have been shown in healthy hearts across differing species. In a limited number of species *ossa cordis* have been associated with cardiovascular disease, such as in cats, dogs and chimpanzees (11, 31, 33). The giraffe in the present study did not present with cardiovascular disease, therefore, it is unlikely that bone formation was influenced by disease processes in this case, indicating a normal anatomical finding, not pathological occurrence.

Bone, cartilage and dystrophic calcification, an accumulation of chemical compounds including calcium phosphate (40), can all present as dense objects in CT scans, therefore histological identification of dense objects is vital. The present study used a variety of histological stains to enable observation of tissue morphology and to identify the cells and fibres within, and surrounding, the cardiac skeleton. Trabeculated bone and bone marrow, alongside vasculature confirmed the µCT dense object was bone, with associated cartilage. Von Kossa staining was used to identify calcium deposits, which can reside in both plaques and bone (41), but this enabled visualization of calcium deposits in the giraffe *ossa cordis*.

Alongside the discovery of *ossa cordis dextrum*, this study also showed the novel discovery of cartilage tissue surrounding the giraffe *ossa cordis dextrum*, as shown by the histological staining. Alcian blue positively identifies acidic polysaccharides, such as glycosaminoglycan present in cartilage (42) and was therefore useful in differentiating bone from the surrounding cartilage in the giraffe. Some chondrocytes appeared to be within the outer regions of the bone itself, similar to that observed in cattle *ossa cordis* (20). This close association may indicate the bone formed via endochondral ossification. Previous studies in the water buffalo, camel, horse, sheep, otter, dog and chimpanzee (6, 12, 13, 19, 33, 43-45) have shown cartilage and/or suggested endochondral ossification as a possible process for *ossa cordis* development due to observations of cartilage in close proximity to bone. *Cartilago cordis*, instead of *ossa cordis*, have been observed in the same anatomical location, and within the same species, mostly in younger animals, where older animals present with *ossa cordis* (6, 8, 11-13, 43, 46). These studies again indicate the possibility of endochondral ossification in this anatomical location within the heart. It is possible cartilaginous cells/foci result in *cartilago cordis*, which may develop into *ossa cordis*. Endochondral ossification also requires involvement of type III collagen. Picrosirius red can be used to differentiate collagen types (11, 24, 47) and was used in this giraffe case to determine rations of collagen

type I versus collagen type III and to describe the staining patterns observed. Following microscopic analysis, the giraffe myocardial tissue surrounding the *ossa cordis* had a much greater proportion of green (likely collagen type III) fibers than myocardial tissue further away from bone (84% compared to 58%). The bone itself was predominantly collagen type I. During chondrogenesis and osteogenesis, levels of differing collagens vary, but once cartilage is ossified type I collagen becomes detectable in ossifying chondrocytes and is present in bone (48, 49). Observations made in the development of another heterotopic bone, the rat *os penis*, showed interstitial bone development can occur by a combination of processes, both endochondral and intramembranous ossification - direct bone formation from mesenchymal tissue (50, 51).

Osteocartilaginous metaplasia in sheep, not *ossa cordis* but located within the myocardium, have also shown evidence of endochondral ossification (52). Given the presence of cartilage in the giraffe, it is therefore possible in this species the giraffe *ossa cordis* develops via a combination of these two processes. Only evidence supporting endochondral ossification was investigated in this study as mature cartilage was present. The present observations included the presence of cartilage tissue, chondrocytes in close proximity to the bone, and the collagen types observed, add supporting evidence to the hypothesis that *ossa cordis* may develop from cartilage via endochondral ossification. This does not exclude possible involvement of intramembranous ossification in *ossa cordis* development.

Osteocalcin is expressed in human cardiomyocytes, vascular endothelial cells, pericytes, vascular smooth muscle cells and other cell types (53). This hormone is the most abundant, non-collagenous peptide found in bone (54). In the giraffe heart, osteocalcin was observed in the *ossa cordis*, cardiomyocytes, and within the associated vasculature. This is the first study to show osteocalcin expression in an *ossa cordis* from any species. Although secreted by osteoblasts, osteocalcin exerts effects on a variety of tissues throughout the body and is involved in many functions ranging from cognitive function through to insulin synthesis (55). One notable function in muscle has been linked to IL-6 secretion, with an IL-6/osteocalcin signaling loop suggested in the literature (56). IL-6 also has many roles producing both anti-inflammatory and proinflammatory effects, with links to coronary artery calcium and cardiovascular disease (57, 58). The novel finding of osteocalcin in *ossa cordis* not only shows similarities with other bones in the body, but also highlights some potential functions relating to inflammation, calcium, and heart disease.

Similar to some other mammals which have *ossa cordis*, the giraffe *ossa cordis dextrum* was found in the anatomical region of the interatrial septum, an area subject to high mechanical stress. This may support the hypothesis that functionally the bone could help protect the heart from shearing under these forces (7). Also residing in this region are the major conductive heart cells and tissues, and therefore the *ossa cordis* may help prevent damage to these critical conductive tissues. This hypothesis was first suggested regarding *ossa cordis* in cattle but has since been suggested following the discovery of *ossa cordis* in sheep and otters as well as supporting evidence from the discovery of *cartilago cordis* in the platypus and many other species (8, 12, 36, 37, 44, 59). It is possible that *ossa cordis* may have more functions. The human cardiac for example, aids the coordination of cardiac contraction by allowing myocardial fibers to insert into it acting as an anchor against contraction (2-4). It is possible that *ossa cordis*, and *cartilago cordis*, also perform this role as suggested in cattle, sheep camels, where cardiomyocytes were found inserting into *ossa cordis* (6, 38, 44). No cardiomyocytes were observed within the *ossa cordis* of the giraffe, they appeared to surround the bone and cartilage, however, this does not rule out the possibility that they play a role in cardiac contraction.

This novel study confirmed the presence of an *ossa cordis dextrum*, surrounded in part by cartilaginous tissue, in a reticulated giraffe and additionally revealed the microstructure of this cardiac bone. It must be recognized this is a case study, further work investigating differing ages and disease states, and increased numbers of individuals, would show prevalence, developmental processes and whether aging or pathological differences alter occurrence and morphology in this species. This work improves our understanding of cardiac anatomy in the giraffe and provides interesting similarities and differences both within the *Artiodactyla* order and other species. The discovery of *ossa cordis* in giraffes, alongside previous findings in cattle, sheep, goat, water buffalo, deer and camels, demonstrates that cardiac bone is a common finding in the *Artiodactyla* order. This poses the question that if more species were investigated, could more novel discoveries of ossa cordis in differing species be made? This could lead to further comprehension regarding phylogeny, formation, function and presentation in different species. This may also help us understand the formation processes of heterotopic cartilage and bone for medical and surgical purposes. Treatments towards preventing, reducing or increasing bone and cartilage growth, both *in vivo* and *ex vivo* for implantation, could all be informed by understanding heterotopic bone and cartilage formation.

Acknowledgements

Funding: The authors would like to thank The University of Nottingham, School of Veterinary Medicine and School of Biosciences. The Hounsfield Facility received funding from European Research Council (Futureroots Project), Biotechnology and Biological Sciences Research Council of the United Kingdom, Natural and Environment Research Council of the United Kingdom and the Wolfson Foundation.

Conflicts of Interest: The authors have no conflicts of interest to declare.

Supplementary Files: Video 1. Giraffe *ossa cordis*. 3D structure and bone density variation. https://figshare.com/s/6bc1303547d80 f103ff4 Video 2. Giraffe *ossa cordis*. 3D structure and bone local thickness. https://figshare.com/s/6bc1303547d80f103ff4

References

1. Anderson, R.H., J. Yanni, M.R. Boyett, N.J. Chandler, and H. Dobrzynski, *The anatomy of the cardiac conduction system.* Clinical Anatomy, 2009. 22(1): p. 99-113.

2. Jorge Carlos Trainini., Mario A. Beraudo., Mario Wernicke., Alejandro Trainini., Jorge A. Lowenstein., Catrin Rutland., et al., *El fulcro cardíaco en la fisiología del corazón helicoidal (The cardiac fulcrum in the physiology of the helical heart)*. 2025, Buenos Aires, Argentina: Editorial Biblos.

3. Trainini, J.C., J. Lowenstein, M. Beraudo, M. Wernicke, A. Trainini, V.M. Llabata, et al., *Myocardial torsion and cardiac fulcrum.* Morphologie, 2021. 105(348): p. 15-23.

4. Trainini, J.C., J.A. Lowenstein, M.A. Beraudo, V.M. Llabata, F. Carreras-Costa, J.V. Cabezas, et al.,*Fulcrum and Torsion of the Helical Myocardium*. 2022, Buenos Aires, Argentina: Editorial Biblos.

5. De Almeida, M.C., D. Sanchez-Quintana, N. Davis, F.R. Charles, A. Chikweto, W. Sylvester, et al., *The ox atrioventricular conduction axis compared to human in relation to the original investigation of sunao tawara.* Clinical Anatomy, 2020. 33(3): p. 383-393.

6. Balah, A., M.H. Bareedy, A.A. Abuel-atta, and W. Ghonimi, *Os cordis of the mature dromedary camel heart (Camelus dromedaries) with special emphasis to the cartilago cordis.* J. Adv. Vet. Anim. Res., 2014. 1(3): p. 130-135.

7. Best, A., M. Egerbacher, S. Swaine, W. Perez, A. Alibhai, P. Rutland, et al., *Anatomy, histology, development and functions of Ossa cordis: A review.* Anat Histol Embryol, 2022. 51(6): p. 683-695.

8. Kubale, V., A. Best, S. Mai, T. Smale, A. Alibhai, W. Perez, et al., *Anatomy, Histology, Aetiology, Development and Functions of Cartilago Cordis: A Systematic Review.* Cells Tissues Organs, 2025. 214(5): p. 366-390.

9. Meyers, C., J. Lisiecki, S. Miller, A. Levin, L. Fayad, C. Ding, et al., *Heterotopic Ossification: A Comprehensive Review.* JBMR Plus, 2019. 3(4): p. e10172.

10. Berendsen, A.D. and B.R. Olsen, *Bone development.* Bone, 2015. 80: p. 14-18.

11. Moittie, S., K. Baiker, V. Strong, E. Cousins, K. White, M. Liptovszky, et al., *Discovery of os cordis in the cardiac skeleton of chimpanzees (Pan troglodytes).* Scientific Reports, 2020. 10(1).

12. Egerbacher, M., H. Weber, and S. Hauer, *Bones in the heart skeleton of the otter (Lutra lutra).* Journal of Anatomy, 2000. 196: p. 485-491.

13. Daghash, S. and H. Farghalil, *The cardiac skeleton of the Egyptian Water buffalo (Bubalus bubalis).* Int. J. Adv. Res. Biol. Sci., 2017. 4: p. 1-3.

14. Owen, R., *Notes on the Anatomy of the Nubian Giraffe.* The Transactions of the Zoological Society of London, 1839. 2(3): p. 217-243.

15. Murie, J., *XX.—On the horns, viscera, and muscles of the Giraffe; with a record of the post mortem examination of two specimens killed by a fire.* Annals and Magazine of Natural History, 1872. 9(51): p. 177-195.

16. Crisp, E., *Further contributions to the anatomy of the giraffe and the nylghau.* Proceedings of the Zoological Society of London, 1864. 1864: p. 269-271.

17. Perez, W., M. Lima, G. Pedrana, and F. Cirillo, *Heart anatomy of Giraffa camelopardalis rothschildi: a case report.* Veterinarni Medicina, 2008. 53(3): p. 165-168.

18. Alsafy, M.A.M., S.A.A. El-Gendy, B.M. Kamal, C.S. Rutland, H.H. Abd-Elhafeez, S. Soliman, et al., *Heart ventricles of the dromedary camel (Camelus dromedarius): new insights from sectional anatomy, 3D computed tomography, and morphometry.* BMC Zoology, 2023. 8(1): p. 12.

19. El-Gendy, S.A.A., M.A.M. Alsafy, C.S. Rutland, S.M. Ez Elarab, H.H. Abd-Elhafeez, and B.M. Kamal, *Ossa cordis and os aorta in the one-humped camel: Computed tomography, light microscopy and morphometric analysis.* Microsc Res Tech, 2023. 86(1): p. 53-62.

20. Alsafy, M.A.M., S.A.A. El-Gendy, B. Atkinson, C.J. Sturrock, B.M. Kamal, A. Alibhai, et al., *Novel Insights Into the Architecture of Macro and Microstructures in Cattle Ossa Cordis.* Microscopy and Microanalysis, 2024. 30(3): p. 574-593.

21. Witkowska, A., A. Alibhai, C. Hughes, J. Price, K. Klisch, C.J. Sturrock, et al., *Computed tomography analysis of guinea pig bone: architecture, bone thickness and dimensions throughout development.* PeerJ, 2014. 2: p. e615.

22. Doube, M., M.M. Klosowski, I. Arganda-Carreras, F.P. Cordelieres, R.P. Dougherty, J.S. Jackson, et al., *BoneJ: Free and extensible bone image analysis in ImageJ.* Bone, 2010. 47(6): p. 1076-9.

23. Schneider, C.A., W.S. Rasband, and K.W. Eliceiri, *NIH Image to ImageJ: 25 years of image analysis.* Nat Methods, 2012. 9(7): p. 671-5.

24. Wilson, J.P., M.J. Green, L.V. Randall, J.N. Huxley, A. Alibhai, H.J. Ferguson, et al., *A history of lameness is associated with reduced proportions of collagen type I relative to type III in the digital cushions of dairy cattle.* J Dairy Sci, 2025. 108(12): p. 13807-13819.

25. Partusch, L., C.S. Rutland, A. Martens, C. Du Cheyne, W. De Spiegelaere, and J.K. Michler, *Collagen composition in equine exuberant granulation tissue reflects tissue immaturity.* PLoS One, 2025. 20(11): p. e0335179.

26. Schindelin, J., I. Arganda-Carreras, E. Frise, V. Kaynig, M. Longair, T. Pietzsch, et al., *Fiji: an open-source platform for biological-image analysis.* Nature Methods, 2012. 9(7): p. 676-682.

27. Brown, T.J., C.S. Rutland, K.K. Choi, F. Tse, M.J. Peffers, N.P. Mongan, et al., *Modulation of the premetastatic bone niche: molecular changes mediated by bone-homing prostate cancer extracellular vesicles.* Frontiers in Cell and Developmental Biology, 2024. Volume 12 - 2024.

28. Alstrup, A.K.O., H. Lauridsen, K. Ydesen, and J.S. Agerholm, *Possible Pregnancy Toxemia in a Late-Term Twin-Pregnant Harbor Seal (Phoca vitulina).* Aquatic Mammals, 2025. 51(3): p. 276-280.

29. Goncalves, T.C., M.C.C. da Costa, R.L. Santana, M.A.S. Ferreira, E.G. Giese, E. Branco, et al., *Cardiac morphology of Phalacrocorax brasilianus.* Anat Rec (Hoboken), 2025.

30. Feio, J.V., M.A.S. Ferreira, E.G. Giese, É. Branco, A.B. Guerreiro Junior, and A.R. de Lima, *Cardiac morphological and morphometric analysis of Ardea alba.* Anat Rec (Hoboken), 2026.

31. Liu, S.K., L.P. Tilley, and R.J. Tashjian, *Lesions of the conduction system in the cat with cardiomyopathy.* Recent Adv Stud Cardiac Struct Metab, 1975. 10: p. 681-93.

32. Yoshida, M., K. Miyoshi, T. Tajima, A. Wada, H. Ueda, and T. Kooriyama, Anatomical features of ossa cordis in the Steller sea lion. J Vet Med Sci, 2022. 84(5): p. 660-665.

33. James, T.N. and E.H. Drake, *Sudden death in Doberman pinschers.* Ann Intern Med, 1968. 68(4): p. 821-9.

34. Dupuy, G., *(The deer's cross) Les Cahiers Cynegetiques Du Naturaliste.* 2011, Grance: Montbel.

35. Endo, H., T. Sakai, T. Itou, H. Koie, and J. Kimura, *Macroscopic observation and CT examination of the heart ventricular walls in the Asian elephant.* Mammal Study, 2005. 30(2): p. 125-130, 6.

36. Frink, R.J. and B. Merrick, *Sheep heart - coronary and conduction system anatomy with special reference to presence of an os cordis.* Anatomical Record, 1974. 179(2): p. 189-199.

37. James, T.N., *Anatomy of sinus node AV node and os cordis of beef heart.* Anatomical Record, 1965. 153(4): p. 361-&.

38. Pour, A.A.M., *Comparative morphometry of the heart in Holstein and a native Iranian cow breeds wth emphasis on the OS cordis.* Indian Veterinary Journal, 2004. 81(7): p. 806-809.

39. Mohammadpour, A.A. and M. Arabi, *Morphological study of the heart and os cordis in sheep and goat.* Indian Veterinary Journal, 2007. 84(3): p. 284-287.

40. Wu, C.Y., J. Martel, and J.D. Young, *Ectopic calcification and formation of mineralo-organic particles in arteries of diabetic subjects.* Sci Rep, 2020. 10(1): p. 8545.

41. Meloan, S.N. and H. Puchtler, *Chemical Mechanisms of Staining Methods: Von Kossa's Technique: What von Kossa Really Wrote and a Modified Reaction for Selective Demonstration of Inorganic Phosphates.* Journal of Histotechnology, 1985. 8(1): p. 11-13.

42. Kumar, G.J. and J.A. Kiernan, *Educational Guide, Special Stains and H & E*. 2010, USA: Dako North America.

43. David, T., *Ossa cordis of the carabao (Bulbus bubalis), .* The Philippine Journal of Animal Industry, 1937. 4(6): p. 521-528.

44. Massari, C., A. Ferreira-Silva, H. Riceti-Magalhães, D. Souza-Silva, and M. Miglino, *Computed tomography examination of the os cordis in a lamb (Ovis aries Linnaeus, 1758).* MVZ Cordoba, 2021. 27(1): p. e2153.

45. Nabipour, A. and M.R. Shahabodini, *Histological study of the atrioventricular node and bundle in the heart of ovine fetus.* Iranian Journal of Veterinary Research, 2007. 8(1): p. 64-70.

46. Matsuda, K., S. Tabata, Y. Kawamura, T. Kurosawa, N. Yoshie, and H. Taniyama, *Ectopic Ossification with Haematopoietic Bone Marrow in the Heart Valves of a Crossbred Heavy Horse.* Journal of Comparative Pathology, 2010. 143(2-3): p. 213-217.

47. Lattouf, R., R. Younes, D. Lutomski, N. Naaman, G. Godeau, K. Senni, et al., *Picrosirius red staining: a useful tool to appraise collagen networks in normal and pathological tissues.* J Histochem Cytochem, 2014. 62(10): p. 751-8.

48. Dessau, W., H. von der Mark, K. von der Mark, and S. Fischer, *Changes in the patterns of collagens and fibronectin during limb-bud chondrogenesis.* J Embryol Exp Morphol, 1980. 57: p. 51-60.

49. Wulf, M., A. Bosse, T. Wiethege, B. Voss, and K.M. Müller, *Localization of collagen Types I, II, and III mRNAs in human heterotopic ossification by non-radioactive in situ hybridization.* Pathology Research and Practice, 1994. 190(1): p. 25-32.

50. Murakami, R., K. Izumi, and I. Yamaoka, *Androgen-dependent and independent process of bone formation in the distal segment of Os penis in the rat.* Eur J Morphol, 1995. 33(4): p. 393-400.

51. Murakami, R., *Development of the os penis in genital tubercles cultured beneath the renal capsule of adult rats.* J Anat, 1986. 149: p. 11-20.

52. Gopalakrishnan, G., W.E. Blevins, and W.G. Van Alstine, *Osteocartilaginous metaplasia in the right atrial myocardium of healthy adult sheep.* Journal of Veterinary Diagnostic Investigation, 2007. 19(5): p. 518-524.

53. Uhlén, M., L. Fagerberg, B.M. Hallström, C. Lindskog, P. Oksvold, A. Mardinoglu, et al., *Tissue-based map of the human proteome.* Science, 2015. 347(6220): p. 1260419.

54. Millar, S.A., H. Patel, S.I. Anderson, T.J. England, and S.E. O'Sullivan, *Osteocalcin, Vascular Calcification, and Atherosclerosis: A Systematic Review and Meta-analysis.* Front Endocrinol (Lausanne), 2017. 8: p. 183.

55. Moser, S.C. and B.C.J. van der Eerden, *Osteocalcin-A Versatile Bone-Derived Hormone.* Front Endocrinol (Lausanne), 2018. 9: p. 794.

56. Chowdhury, S., L. Schulz, B. Palmisano, P. Singh, J.M. Berger, V.K. Yadav, et al., *Muscle-derived interleukin 6 increases exercise capacity by signaling in osteoblasts.* J Clin Invest, 2020. 130(6): p. 2888-2902.

57. Feng, Y., D. Ye, Z. Wang, H. Pan, X. Lu, M. Wang, et al., *The Role of Interleukin-6 Family Members in Cardiovascular Diseases.* Front Cardiovasc Med, 2022. 9: p. 818890.

58. Ahmad, M.I., P.A. Chevli, S. Mirzai, R. Rikhi, N. Pagidipati, L. Slipczuk, et al., *Relationship between interleukin-6, coronary artery calcium and risk of heart failure: Insights from MESA.* American Journal of Preventive Cardiology, 2025. 24: p. 101310.

59. Davies, F., *The conducting system of the monotreme heart*, in *Anatomy Department*. 1931, King's College London: London, UK.

C. J. Sturrock, A. Best, A. Alibhai, J. Jackson-Oxley, J. J. Jeyapalan, B. Atkinson, W. Perez, C. S. Rutland

Izvleček:

Ključne besede: